Fuel 382 (2025) 133712

Contents lists available at ScienceDirect

Fuel

journal homepage: www.elsevier.com/locate/fuel

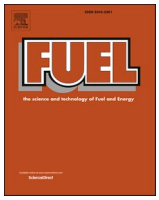

Full Length Article

Pragmatic investigation of the effect of ether additives on biodiesel combustion to reduce NO_x and other harmful emissions

Arun Teja Doppalapudi [a], Abul Kalam Azad [a,*], Md Nurun Nabi [a], Mohammad G. Rasul [b], Mohammad Masud Kamal Khan [c]

[a] School of Engineering and Technology, Central Queensland University, Melbourne Campus, 120 Spencer Street, Melbourne, VIC 3000, Australia
[b] School of Engineering and Technology, Central Queensland University, Rockhampton, QLD 4702, Australia
[c] School of Engineering, Computer & Mathematical Sciences, Auckland University of Technology, Auckland, New Zealand

ARTICLE INFO

Keywords:
Biodiesel
NO_x emissions
Diethyl ether
Diethylene glycol dimethyl ether
Tri-propylene-glycol monomethyl ether
Oxygenated additives

ABSTRACT

The addition of oxygenated additives such as ethers has shown better results with improved combustion and reduced emissions. Ethers have a lower viscosity and higher oxygen concentrations that can improve combustion and have lower calorific value, which can control the cylinder temperature. Hence, three ethers: diethyl ether (DEE), Diethylene Glycol Dimethyl Ether (DME), and Tri-propylene-Glycol Monomethyl ether (TME) were selected as biodiesel additives to conduct engine tests for reducing NO_x and CO emissions. These three ethers were added at 10 % volume to the Tucuma B10 blend, and the results were compared with diesel, TB10, and TB20. The performance, combustion, and emission characteristics were investigated through engine tests conducted at 2400 rpm with varying loads of 25 %, 50 %, 75 %, and 100 %. The study found that adding oxygenated additives into the TB10 blend has led to a decrease in both CO and NO_x compared to the TB10 blend alone. However, the NO_x was higher for the ether-TB10 blends than diesel. At full load, TB10DME10 reduced CO emissions by 22.3 %, 45 %, and 38 %, compared to diesel, TB10, and TB20, respectively. Also, TB10TME10 showed reduced NO_x by 8.5 %, 5.2 %, 6.62 %, and 0.12 % compared to TB10 at 25 %, 50 %, 75 %, and 100 % loads, respectively. Peak pressure values for ether blends were lower than diesel but higher than TB10 and TB20. The study concluded that the TB10DEE10 has shown better results in reducing CO, NO_x, and BSFC and improved BTE. The study recommends a detailed computational fluid dynamics study to investigate more combustion aspects of ether blends. In addition, further investigation on oxidative stability, tribological behaviour, and cold flow performance of the ether blends is much needed.

1. Introduction

Over the years, the transportation sector has depended on petroleum-based fuels and is responsible for higher carbon monoxide (CO), hydrocarbons (HC), nitrogen oxides (NO_x) and particulate matter (PM) emissions [1,2]. Large, heavy machinery used in mining, manufacturing, and marine sectors uses diesel engines, which are highly responsible for NO_x and PM emissions. These emissions are harmful to the environment and human health [3–5]. For instance, According to World Energy Outlook 2023 by the International Energy Agency IEA [6], the energy sector is predominantly responsible for the contaminated air that affects over 90 % of the global population, contributing to over 6 million premature deaths annually [6]. Additionally, in 2015, it was estimated that fine particulate matter (PM2.5) in outdoor air was responsible for 4.2 million deaths and 103.1 million disability-adjusted

Abbreviations: BDC, Bottom dead center; BP, Brake power; BTE, Brake thermal efficiency; BSFC, Brake-specific fuel consumption; CO, Carbon monoxide; CO_2, Carbon dioxide; CHRR, Cumulative heat release rate; DBE, Dibutyl ether; DEE, Diethyl ether; DMM, Dimethoxy methane; DME, Diethylene glycol dimethyl ether; EVC, Exhaust valve closing; EVO, Exhaust valve opening; HC, Hydrocarbons; HRR, Heat release rate; ICP, In-cylinder pressure; IEA, International energy agency; IMEP, Indicated mean effective pressure; IP, Indicated power; ISFC, Indicated specific fuel consumption; IVC, Intake valve closing; IVO, Intake valve opening; MGO, Marine gas oil; NO_x, Nitrogen oxides; PM, Particulate matter; ROPR, Rate of pressure rise; SOC, Start of combustion; TB10, 10% Tucuma and 90% diesel by volume; TB20, 20% Tucuma and 80% diesel by volume; TB10DEE10, 10% Tucuma, 10% diethyl ether and 80% diesel by volume; TB10DME10, 10% Tucuma, 10% Diethylene-Glycol Dimethyl ether and 80% diesel by volume; TB10TME10, 10% Tucuma, 10% Tri Propylene-Glycol Monomethyl ether and 80% diesel by volume; TDC, Top dead centre; TME, Tripropylene-Glycol Monomethyl ether.

* Corresponding author.
E-mail address: a.k.azad@cqu.edu.au (A.K. Azad).

https://doi.org/10.1016/j.fuel.2024.133712
Received 29 July 2024; Received in revised form 8 October 2024; Accepted 9 November 2024
Available online 14 November 2024

Nomenclature

Symbol	Description
A	Area of piston (m^2)
dp	Change in pressure
dv	Change in volume
$d\theta$	Change in crank angle
L	Stroke length (m)
N	Speed (rpm)
Q_{net}	In-cylinder heat release rate
γ	Ratio of specific heats
p	In-cylinder pressure (Pa)
v	In-cylinder volume in (m^3)
λ	The ratio of connecting rod length to crankshaft

life-years [7,8]. Implementing biodiesel in diesel engines has significantly reduced CO, HC, sulfur oxides, and PM emissions. However, NO_x emissions are higher with biodiesel-fuelled engines than diesel-fuelled engines. Although biodiesel and conventional diesel fuel share many characteristics, differences in their physicochemical properties lead to variations in combustion. Blending biodiesel and diesel blends with oxygenated fuels can reduce the blend's total viscosity and improve the combustion process.

Blending biodiesel with oxygenated additives such as ethers showed better results in reducing the viscosity of the blend and improving the combustion [9,10]. Ethers such as dibutyl ether (DBE), Diethylene Glycol Dimethyl Ether (DME), dimethoxy methane (DMM), diethyl ether (DEE), and tripropylene-Glycol Monomethyl ether (TME) were widely investigated to improve the combustion rates [11]. For instance, as per the studies by Abebe Debella et al. [12] and El-Zohairy et al. [13], the kinematic viscosity of the diethyl ether (DEE) at 40 ℃ is 0.23 cSt. The studies revealed that blending DEE with biodiesel has reduced the overall viscosity and improved the spray behaviour. Ethers have a low calorific value and high oxygen content, which makes them suitable for oxidizing CO emissions and reducing the in-cylinder temperature, thereby reducing the NO_x. In one study, Yesilyurt and Aydin [14] observed that the average CO emissions for B20DEE2.5 and B20DEE5 were reduced by 31.86 % and 32.29 % compared to diesel fuel and by 21.79 % and 22.47 % compared to the B20 blend, respectively. In another study, Swaminathan and Sarangan [15] observed a decrease in NO_x by 31 % with the addition of DME to the B20 at lower loads, and increased NO_x was observed at higher loads. DME, also known as diglyme, is characterized by high oxygen content, excellent solubility with diesel fuel, a high cetane number, reduced sooting tendency, and better physical–chemical properties that make it suitable for use in commercial diesel engines [16]. The addition of DME to diesel fuel resulted in reduced emissions of HC, CO, PM, smoke, and soot [17–20], while NO_x emissions could either increase, decrease, or remain nearly unchanged [17,18,21]. Nabi and Hustad [22] tested Marine Gas Oil (MGO) as the base fuel for engine experiments and blended it with 10 % DME (Ox10) and jatropha oil methyl ester (B10). The study revealed that at all engine loads, fine particle number and mass emissions were considerably lower in B10 and Ox10 fuels compared to MGO fuel, with CO emissions reduced by 13 % and 21 %, respectively. MGO has properties that closely resemble those of diesel fuel, and the blended fuels exhibit higher cetane numbers and similar density, viscosity, and calorific values. Oxygenated additives like ethers improve the performance of blended fuels because of their inherent properties, such as increased stability, lower viscosity, higher cetane numbers, and natural oxygen content [23]. For example, Sun et al. [24] observed an increase in BTE and shorter ignition delay with the addition 5 % DME to the biodiesel blend. In addition, Ashfaque Ahmed et al. [25] observed a 5.8 % increase in BTE, a 6.89 % decrease in BSFC, 37.8 % and 50.7 % decrease in CO and HC, respectively, for 20 % blended DEE to the animal fat biodiesel compared to diesel. Hence addition of ethers helps to lower exhaust emissions and improve engine combustion. Therefore, this study examined the impact of these ethers on the biodiesel blends.

In the author's previous studies with the Tucuma blends Doppalapudi et al. [26] and Doppalapudi et al. [27], TB10 has shown better results in terms of improved performance and reduced emissions compared to TB20 and diesel. Considering these findings, the effects of blending CNTs, ethanol, and essential oils with TB10 were studied, revealing that the oxygenated alcohols significantly reduced NOx emissions. To explore this further, ether additives were incorporated into the TB10 blend for a more in-depth analysis of oxygenated fuel combustion in diesel engines. In the current study, engine performance, combustion, and emission parameters were analysed using diesel fuel, a Tucuma-diesel blend (TB10 and TB20), and a TB10 blend with ethers DEE, DME, and TME. The main reason for selecting these three ethers is their higher oxygen content. For instance, the oxygen content in DEE is 21.6 % by wt., whereas for DME and TME, the oxygen content is 35.83 % by mass, containing 31 % by mass, respectively [17,28]. Moreover, the cetane number of the ethers DME (greater than 86), DME (126), and TME (65.0) are higher than diesel (53) [29,30]. DME is widely used as a solvent for the conversion of olefins and the synthesis of other chemicals. Meanwhile, TME is used as a solvent in the resins, coatings, and textile industries. Besides, DEE, DME, and TME were used as internal combustion engine fuels. These variations have motivated authors to explore the effect of these ethers on the combustion aspects with the novel Tucuma blend. The aim was to assess the impact of adding ethers to diesel–biodiesel blends on these parameters, focusing on the influence of oxygen content. This investigation highlighted significant reductions in all diesel engine emissions, including CO, CO_2, HC, and NO_x emissions. The detailed methodology for the experiment and results are discussed in the following sections. Finally, the study concludes the key outcome and is followed by recommendations for future work.

2. Methodology

2.1. Materials used

The study on the effect of different types of ethers on Tucuma biodiesel (TB) involves a series of stages and various materials. For the transesterification process, Amazonian-based Tucuma bio-oil was purchased from Nature in Bottle, U.S.A. In addition, potassium hydroxide (KOH) was used as the catalyst, and methanol was the reacting agent; both were obtained from Westab Pty Ltd, Australia. Ethers such as DEE (CAS:60-29-7) with $\geq$ 99.7 % purity, DME (CAS:111-96-6) with 99.5 % purity, and TME (CAS: 25498-49-1) with $\geq$ 99.7 purity were purchased from Sigma Aldrich, Australia. Finally, diesel fuel for the fuel blends and engine testing was sourced from Ampol Petroleum Company in Queensland, Australia.

2.2. Biodiesel conversion procedure, property analysis, and blend preparation

Firstly, fatty acid methyl esters (FAME) were produced from Tucuma bio-oil using the transesterification process [31]. This process involves mixing alcohols and fatty acids at controlled temperatures and reaction times to convert them into FAME (biodiesel) and glycerol as a byproduct. The yield of FAME depends on the transesterification operating conditions [32]. For instance, Devaraj et al. [33] converted waste cooking oil to high-quality FAME at 75 °C, 1 wt% catalyst concentration, a 1:6 oil-to-methanol molar ratio, 350 rpm, and a reaction time of 90 min, 97 % of the potential biodiesel output was achieved. In another study, Encinar et al. [34] observed maximum methyl ester content ranging from 97-98 % under the conditions of a 9:1 methanol-to-oil molar ratio, 0.7 wt% KOH, a 1:1 co-solvent-to-methanol molar ratio, 700 rpm, and 3 h of reaction time. Hence, the optimization process was

undertaken to convert the Tucuma bio-oil to biodiesel. The experiment was designed using the Box-Behnken method, and the results were analyzed with Response Surface Methodology (RSM). Statistical optimization involved conducting a total of 27 experiments with varying process parameters: methanol-to-oil molar ratio (ranging from 5:1 to 7:1), reaction time (from 50 to 70 min), catalyst concentration (from 0.5 wt% to 1.5 wt%), and reaction temperature (from 50 °C to 70 °C) [27]. The detailed methodology, design of experiments, RSM and ANOVA analysis of Tucuma biodiesel conversion process can be found in authors previous study Doppalapudi et al. [35].

The RSM statistical investigation identifies the optimal conditions to be a methanol-to-oil molar ratio of 7:1, a KOH catalyst concentration of 0.5 % (w/w), a 70-minute reaction time, and a temperature of 53 °C, resulting in a 99.5 % yield conversion. AOCS Ce 1a-13 testing standard was followed to investigate the fatty acid methyl esters (FAME) composition in gas chromatography and mass spectrometry (GCMS) equipment. The analysis revealed that TB biodiesel is mainly composed of oleic acid (44.87 %), palmitic acid (25.69 %), linoleic acid (12.56 %), and stearic acid (11.8 %) fatty esters [26].

Biodiesel blends were created using fossil diesel as the baseline fuel, and the oxygenated fuels varied in percentage volume. The blends include TB10 (10 % Tucuma and 90 % diesel by volume), TB20 (20 % Tucuma and 80 % diesel by volume), TB10DEE10 (10 % Tucuma, 10 % diethyl ether and 80 % diesel by volume), TB10DME10 (10 % Tucuma, 10 % Diethylene-Glycol Dimethyl ether and 80 % diesel by volume) and TB10TME10 (10 % Tucuma, 10 % Tri Propylene-Glycol Monomethyl ether and 80 % diesel by volume). The blends were rigorously mixed in 4-liter batches using a 5-liter conical flask on a magnetic stirrer. The blends were prepared for 60 min with stirring speed maintained at 500 rpm, and the temperature was at approximately 26 ± 1.5 °C.

2.3. Engine test setup

Table 1 shows the specifications of the KubotaV3300 engine and the parameter range and sensitivities of the emission parameters. A full-scale, 4-cylinder, four-stroke Kubota V3300 commercial engine was used for the engine tests, coupled with an eddy current dynamometer to perform the loading. The dynamometer from Dyno Dynamics applied the load on the engine, where the electric motors are used to apply the load on the engine. The highest load was taken as a reference under full-throttle conditions, after which the load values were varied accordingly.

Measurements of engine brake torque, speed, and fuel mass flow rates were taken at each test. Later, standard equations were used to calculate performance parameters, such as brake power (BP), indicated power (IP), indicated mean effective pressure (IMEP), brake thermal efficiency (BTE), indicated specific fuel consumption (ISFC), and brake-specific fuel consumption (BSFC). A piezoelectric pressure transducer was installed on the cylinder head to measure the chamber pressure variations and minimise the noise output (model H32218-GPA from Optrand, MI, USA). The recorded in-cylinder pressure readings are the average of 200 hundred consecutive cycles (from 0 °CA to 720 °CA). A CODA exhaust gas analyser (Andros 6241A, California, USA) was used to measure emissions. This device utilizes nondispersive infrared technology to accurately determine levels of CO, CO_2, HC, and NO_x. [36]. Fig. 1 illustrates the engine test setup and methodology used for evaluating the ether biodiesel blends.

The engine was tested under four different loading conditions, including low load (25 % of total load), medium load (50 % of full load), and high loads (75 % and 100 % of full load). Furthermore, the engine was kept constant at 2400 rpm, close to the rated power rotational speed. The tested fuels in this investigation include neat diesel fuel, which is considered a reference fuel. The properties of pure biodiesel, diesel and ethers were tested by the authors in their previous studies. However, the blended fuels such as TB10DEE10, TB10DME10 and TB10TME10 were calculated as per the proportions of the fuels in their total blends. The properties of the tested fuels are displayed in Table 2. The three oxygenated additives were selected to enhance the combustion and reduce the emissions. Another key reason for choosing these additives is due to the higher oxygen percentage in their molecular structures and superior ignitability. Among all, the blended fuels are under the ASTM D6751 standards, as presented in Table 2.

2.4. Theoretical equations for the engine performance and combustion evaluation

2.4.1. Performance characteristics

Indicated power (IP) is the available energy after a portion of the energy is lost through the coolant, exhaust, and radiation. IP is calculated using indicated mean effective pressure (IMEP) using Equation (1).

$$IP = \frac{IMEP \times L \times A \times \left(\frac{N}{n}\right) \times C \times 100}{60} (kW) \quad (1)$$

Where IMEP is in bar recorded from the combustion analysis, L is the stroke length in meters (m), A is the area of the piston (m^2), N represents the speed in rpm, n value is 2 for four-stroke CI engines, and C value is 4, which denotes the total number of cylinders.

Indicated specific fuel consumption (ISFC) is the ratio of fuel consumption to the indicated power, which can be calculated using Equation (2) [38].

$$\frac{\text{Fuel mass flow rate } \left(\frac{kg}{hr}\right)}{IP\ (kW)} (kg/kW.h) \quad (2)$$

The equations to calculate BP and BSFC were taken from the author's earlier studies Doppalapudi et al. [26] and Doppalapudi et al. [27].

2.4.2. Combustion characteristics

The in-cylinder heat release rate (HRR) was determined from the pressure data and volume data based on the first law of thermodynamics, which is presented in Equation (3) [37,39–41].

Table 1
Technical specifications of the engine and emission analyzer.

Specification of the Kubota V3300		Parameter range and Accuracy of emission analysers	
Engine model and cylinder	Kubota V3300-4 cylinder	Parameter (range)	Accuracy
Compression ratio (CR)	22.6	CO_2 (0–20 %vol)	±0.3 % abs
Bore x stroke (inch)	3.86 × 4.33	O_2 (0–25 %vol)	±0.1 % abs
Injection pressure	13.73 Mpa	HC (0–3000 ppm vol)	±4 ppm abs
Displacement	202.48 cu. in	NO_x (0–5000 vol ppm)	±20 ppm abs
Top clearance	0.0283 in	CO (0–15 %vol)	±0.02 % abs
Intake valve opening	14° Before TDC		
Intake valve closing	36° after BDC		
Injection timing	16 °CA before TDC		
Exhaust valve opening	45° before BDC		
Exhaust valve closing	17° after TDC		

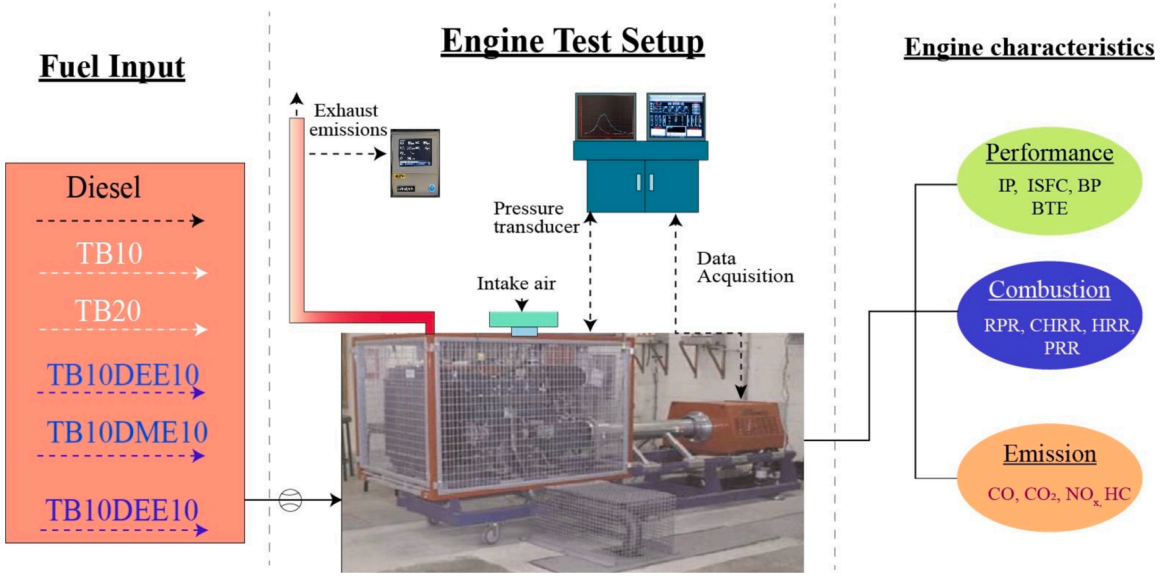

Fig. 1. Experimental procedure for the engine test.

Table 2
Physiochemical properties of the tested fuel blends.

Property	Tucuma B100 [35]	Diesel [37]	TB10	TB10DEE10	TB10DME10	TB10TME10	ASTM ASTM D6751 standard limit [37]
Density (15 °C) in kg/m^3	879.1	832	874.39	863.48	881.48	883.68	860–890
Viscosity (40 °C) in mm^2/s	4.0	4.1	4.01	3.93	3.78	3.95	3.5–5.0
Calorific value in MJ/kg	39.87	41.77	41.58	40.80	39.85	40.41	–
Cetane index	48.2	44	47	52	55	49	Min^m 47

$$\frac{dQnet}{d\theta} = \frac{\gamma}{\gamma - 1} p \frac{dV}{d\theta} + \frac{1}{\gamma - 1} v \frac{dP}{d\theta} \tag{3}$$

Where Q_{net} is the in-cylinder heat release rate (J/°CA), p is the in-cylinder pressure (Pa), v is the instantaneous in-cylinder volume in (m^3), and γ is the ratio of specific heats.

The instantaneous volume was calculated using Equation (4) and Equation (5), where the volume of the cylinder varies with the crank angle position.

$$V = V_c + A.r\left[1 - \cos(\frac{\pi\theta}{180}) + \frac{1}{\lambda}\left(1 - \sqrt{1 - \lambda^2 \sin^2(\frac{\pi\theta}{180})}\right)\right] \tag{4}$$

$$\frac{dV}{d\theta} = \frac{r\pi\theta}{180} \times \left[\sin(\left(\frac{\pi\theta}{180}\right) + \frac{\lambda^2 \sin^2(\frac{\pi\theta}{180})}{2 \times \sqrt{1 - \lambda^2 \sin^2(\frac{\pi\theta}{180})}}\right] \tag{5}$$

V is the instantaneous volume, V_c is the clearance volume, A is the area of cylinder, r is the crank radius, and l is the connecting rod length and λ is the l/r

Cumulative heat release rate is investigated to characterize the efficiency of the combustion process and can be calculated using Equation (6) [42].

$$\text{CHRR} = \int dQ_{net} \tag{6}$$

where Q_{net} is the in-cylinder heat release rate (J/°CA) as presented in Equation (3).

2.5. Uncertainty analysis

To reduce measurement errors, the data was recorded at three different time intervals, and the emissions and performance parameters for each fuel were measured. The potential sources of uncertainty in the results include variations in sensor selection, data measurement, measurement procedures, and instrument calibration. The total experimental uncertainty in this study was determined using the square root method (following the studies [43–45]), as described in equation (7). A total ± 1.88 error is recorded for the experimental setup, which is within the confidence level to evaluate the results.

$$U_o = \sqrt{U_{FC}^2 + U_{BSFC}^2 + U_{BMEP}^2 U_{BTE}^2 + U_{HC}^2 + U_{CO_2}^2 + U_{CO}^2 + U_{NO_x}^2 + U_\lambda^2 + U_{HRR}^2 + U_{CP}^2 + + U_{EGT}^2} \tag{7}$$

$$= \sqrt{(0.10)^2 + (0.70)^2 + (0.2)^2 + (0.90)^2 + (0.30)^2 + (0.02)^2 + (0.80)^2 + (0.10)^2 + (0.8)^2 + (0.05)^2 + (0.90)^2 + (0.02)^2}$$

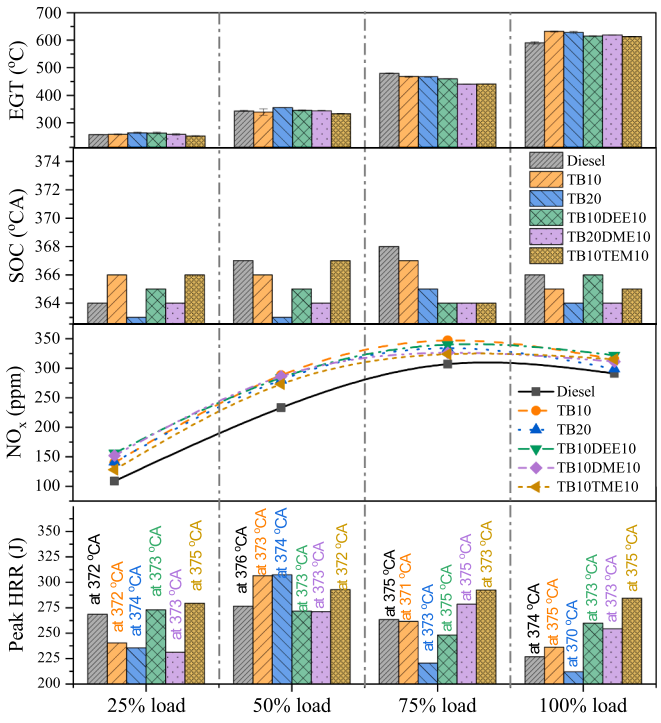

Fig. 2. Effect of heat release rate and early combustion on the NO_x emissions.

$= \pm 1.88\,\%$

3. Results and discussion

3.1. Effect of biodiesel and ether blends on emission characteristics

3.1.1. Effect of biodiesel and ether blends on NO_x emissions

Fig. 2 demonstrates the effect of the start of combustion (SOC) and peak heat release rates (HRR) on NO_x emissions. The premixed combustion stage influences the formation of NO_x emissions, and the rate of premixed combustion is affected by the SOC [37]. Higher peak temperatures are formed during the premixed combustion stage. Factors like air–fuel ratio and fuel calorific value significantly impact this stage, influencing the formation of elevated HRR [46,47]. NO_x emissions increased from 25 % load to 75 % load and decreased to 100 % load. A similar pattern was also observed in the literature by Avase et al. [48] and Khoa and Lim [49]. As presented in Fig. 2, the NO_x trend closely matches the SOC. For instance, reference diesel SOC timing increases from 25 % to 75 % loads and decreases to 100 % load. A similar SOC trend is also observed with TB10 and TB20; however, with the ether blends, the trend is similar but with minor variations. This suggests that NO_x emissions are directly related to the SOC. TB10 showed a higher NO_x trend than all the biodiesel-ether blends, including TB20. TB10 showed increased NO_x emissions by 2.8 %, 3.89 %, and 5.35 % compared to TB20 at 50 %, 75 % and 100 % load conditions, respectively. This is due to the higher calorific value of the fuel, which has increased the combustion temperatures [50]. At 100 % load, the DEE ether blend exhibited higher NO_x than other biodiesel blends. Among all the biodiesel blends, TB10TME10 showed lower NO_x with 128 ppm, 273 ppm, 324 ppm at 25 %, 50 %, and 75 % loads and however, the emissions were more for the same blend at 100 % load condition. In addition, as presented in Fig. 2, EGT is increasing with the increasing load condition [51]. At 25 %, 50 % and 100 % load conditions, biodiesel blends showed higher EGT compared to diesel. At 100 % load, TB10, TB20, TB10DEE10, TB10DME10, and TB10TME10, showed 632℃, 628 ℃, 615 ℃, 619 ℃, and 613 ℃, whereas diesel showed 590 ℃. The addition of ethers to the biodiesel has reduced the EGT compared to TB10 and TB20. Hence, the addition of ethers showed a reduced EGT compared to biodiesel-diesel blends.

Fig. 3 presents the effect of ethers on the NO_x emissions with the biodiesel blends at varying load conditions. As can be seen from Fig. 3, the presence of oxygenated ethers in the TB10 has increased the NO_x emissions compared to diesel at all the load conditions. For instance, the presence of DEE blend in TB10 showed an increase in NO_x by 43.11 %, 21.88 %, 10.74 %, and 10.65 % compared to diesel at loads 25 %, 50

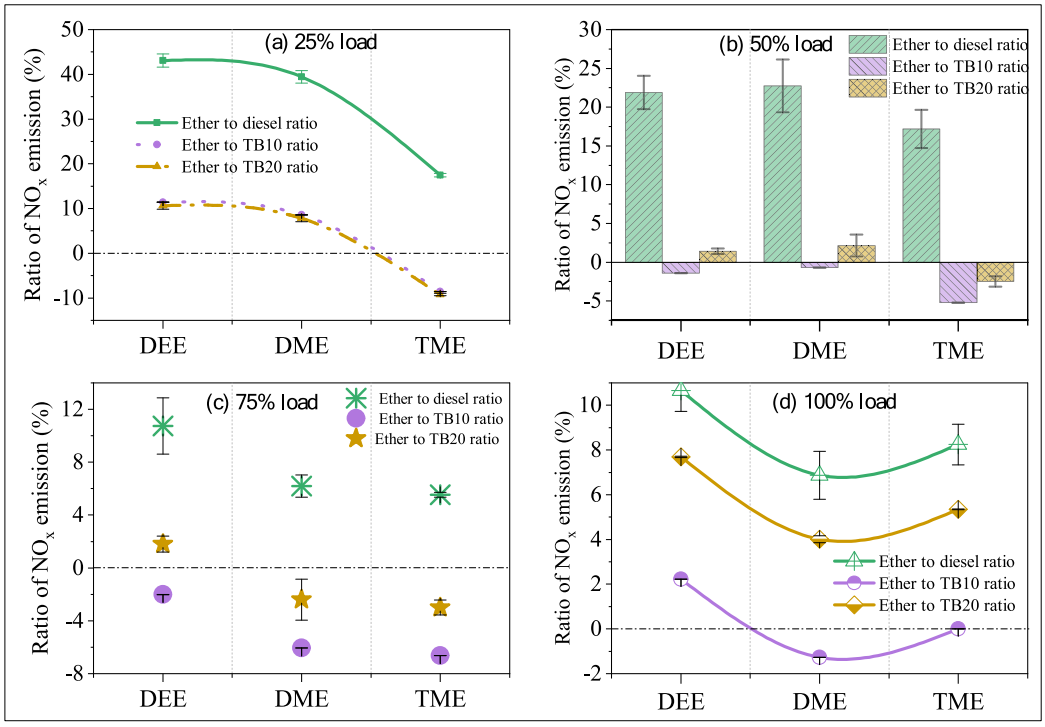

Fig. 3. Effect of TB10-ether blends on NO_x emissions compared to diesel, TB10 and TB20.

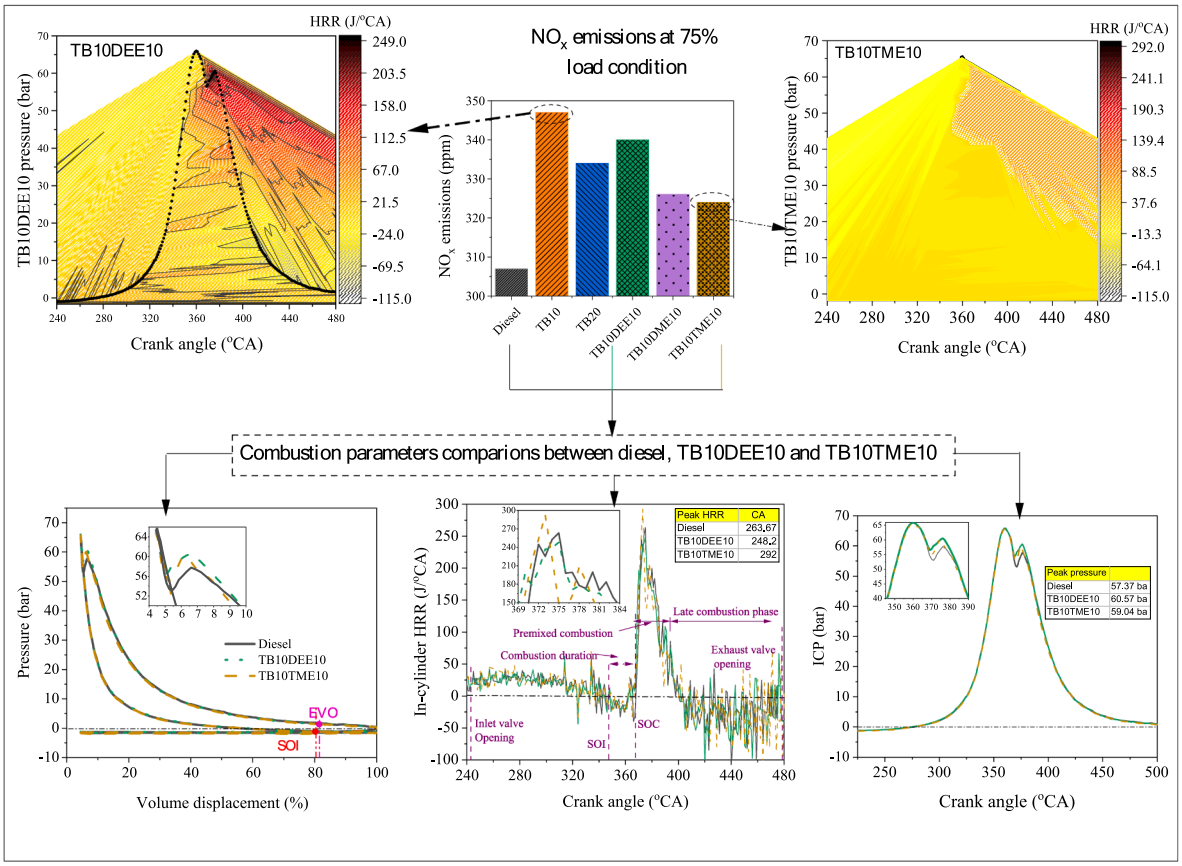

Fig. 4. Comparison of NO_x emissions with the combustion parameters.

%,75 %, and 100 %, respectively. At 50 % load, the DME blend with TB10 showed higher NO_x than all the blends, which is 22.7 % higher than diesel at that respective load. TME blend has shown lower NO_x compared to TB10 and TB20. As shown in Fig. 3(a), at 25 % load condition, the TB10TME10 blend reduced NO_x by −8.6 % and −9.2 % compared to TB10 and TB20, respectively. At 50 % load conditions (Fig. 3 (b)), all the ether blends TB10DEE10, TB10DME10, and TB10TEE10 showed reduced NO_x by −1.4 %, −0.6 % and −5.2 %, respectively, compared to TB10. However, the DEE and DME blends revealed an increased NO_x of 1.4 % and 2.1 % compared to TB20 under the same load conditions. Also, Fig. 3(c) and 3(d) show that DME and TME have shown more reductions in NO_x compared to DEE. DEE has shown higher NO_x because of the blend's lower viscosity, lower density, and higher calorific value. For example, Sezer [52] noted a reduction in NO_x emissions with the DEE blend compared to the DME when operated at different equivalence ratio conditions. The study revealed lower in-cylinder temperatures were formed with the ether-blended fuels. Similar findings were observed in studies by Agarwal et al. [53] and Rakopoulos et al. [54].

Fig. 4 demonstrates the impact of combustion parameters on NO_x formations. Fig. 2 depicts that higher NO_x emissions are observed at a 75 % load condition, and Fig. 3 shows that DEE and TME have considerable variations in the NO_x. TB10DEE10 and TB10TME10 were selected to compare the NO_x and combustion parameters. NO_x emissions are mainly due to the higher temperatures inside the chamber [55,56]. The pressure is directly proportional to the temperature. The higher pressure was recorded for TB10DEE10 (60.57 bar), followed by TB10TME10 (59.04 bar) and diesel (57.37 bar). Hence, the higher NO_x is noted in the order of TB10DEE10 (340 ppm), followed by TB10TME10 (324 ppm) and diesel (307 ppm). Though the pressure–velocity (PV) plot revealed higher pressure at lower volume (near TDC), due to the consequence of

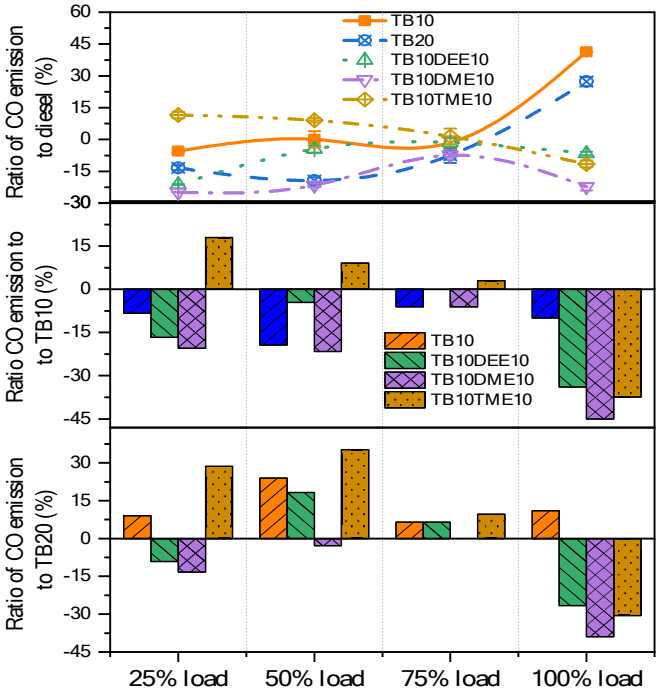

Fig. 5. Variation of CO emissions for the biodiesel and ether blends compared to diesel, TB10 and TB20 blends.

finite time combustion, the combustion peak pressure occurs after the TDC during combustion stroke. From the second peak of the PV graph, higher peak pressure rise rates were observed for the TB10DEE10 than TB10TME10. TB10TME10 has shown higher HRR than the diesel and TB10DEE10. Interestingly, a sudden rise in peak and a sudden drop in the heat release rate can be observed compared to the TB10DEE10. Hence, this phenomenon has caused a drop in the temperature rates inside the chamber and has caused lower NO_x emissions [57–59].

3.1.2. Effect of biodiesel and ether blends on CO emissions

Fig. 5 demonstrates the effect of ethers on the CO emissions. Fig. 5(a) shows the variation of CO emissions for biodiesel blends compared to diesel. Fig. 5(b) and 5(c) show the variation in CO of ester blends compared to TB10 and TB20, respectively. CO emissions are mainly produced due to incomplete combustion and lack of oxygen in the combustion chamber [43]. Combustion events are highly sensitive as there is a greater chance for incomplete combustion depending on the operating range. Carbon atoms are first formed as CO rather than CO_2 emissions during combustion because carbon is more susceptible to the nearby available oxygen. This is one of the major reasons CO can harm human health. Upon inhalation, it absorbs blood oxygen and can cause blood clots in the human body [60]. However, higher temperatures and more oxygen are required to oxidize the CO to CO_2 emissions [61,62]. For example, in Fig. 5, it is noticed that CO emissions first decrease with the increasing load to 75 % load condition and then increase at the full load condition. Similar findings were depicted in studies by Raman et al. [63], Simsek and Uslu [64], EdwinGeo et al. [65], and Simsek [66]. The rate of oxidation increases due to the increase in cylinder temperature conditions as the load increases. However, a sudden rise in emissions is noticed at full load conditions, which means significant amounts of fuel get injected in the high load condition [65]. Hence, there is limited time for the fuel to disperse, atomise, vapourise, combust and oxidise at that condition. In a way, the fuel properties influence both of these factors, such as time and higher quantities of fuel.

Fuel properties have a direct impact on the CO emissions [67]. For instance, as shown in Fig. 5, CO emissions are lower for biodiesel and ether blends than for diesel. Biodiesel has readily available oxygen upon combustion, oxidising CO to CO_2 emissions. Air intake also plays a decent role in supplying oxygen for combustion. For example, passing the exhaust gas recirculated to the combustion has increased CO emissions even when using oxygenated blends [68–70]. This concludes the influence of air intake on CO emissions. CO emissions are lower for the TB10 blend than TB20, as higher quantities of oxygen are available in TB20 than in TB10. Despite the higher oxygen content, both blends showed higher CO at 100 % load than diesel. At 100 % load, CO emissions are 122 ppm,172 ppm,150 ppm,112 ppm, 99 ppm and 104 ppm for the diesel, TB10, TB20, TB10DEE10, TB10DME10, and TB10TME10, respectively. There are several reasons behind these variations. The higher acid value of the Tucuma biodiesel is one of the primary reasons for the higher CO emissions. Also, large quantities of biodiesel cause poorer air–fuel mixture formation at 100 % load conditions, leading to higher CO emissions. However, adding ethers has decreased the CO emissions at higher load conditions. However, at 25 % and 50 %, TB10TME10 showed a 25 % and 38 % increase in CO emissions compared to TB20. However, at higher loads, a decrease in CO emissions is noted for the ether blended fuels.

Adding 10 % by vol. of ethers to the TB10 blend has decreased the CO emissions at 100 % load conditions. The addition of DME has reduced the CO by 22.3 %, 45 %, and 38 %, compared to diesel, TB10, and TB20, respectively, at 100 % load condition. Similarly, TB10DEE10 and TB10TME10 showed reduced CO by 6 % and 11 % with diesel, 34 % and 37 % with TB10, and 26.6 % and 30.52 % with TB20, respectively. Among all, DME10 has shown better emissions reductions than others, including pure biodiesel blends.

3.1.3. Effect of biodiesel and ether blends on CO_2 emissions

Fig. 6 presents the rate of CO_2 emissions for the Tucuma and ether blends at varying loads. CO_2 increases with the increasing load conditions due to the higher oxidation rates formed by higher cylinder temperatures. A similar trend was also noticed in the study by Simhadri et al. [71]. Biodiesel blends showed higher CO_2 emissions than diesel due to readily available oxygen in the biodiesel structure. This is due to the presence of higher oxygen, where the fuel is burned more thoroughly, resulting in the production of water and CO_2 by the end of the reaction [72]. In addition, parameters such as fuel properties, engine speed/load, the C/H ratio, fuel pressure, mixture density, and the timing of injection also influence the rate of CO_2 formation [73,74]. Compared to TB20, TB10 has shown higher CO_2 emissions. TB10 showed a 16 % increase in

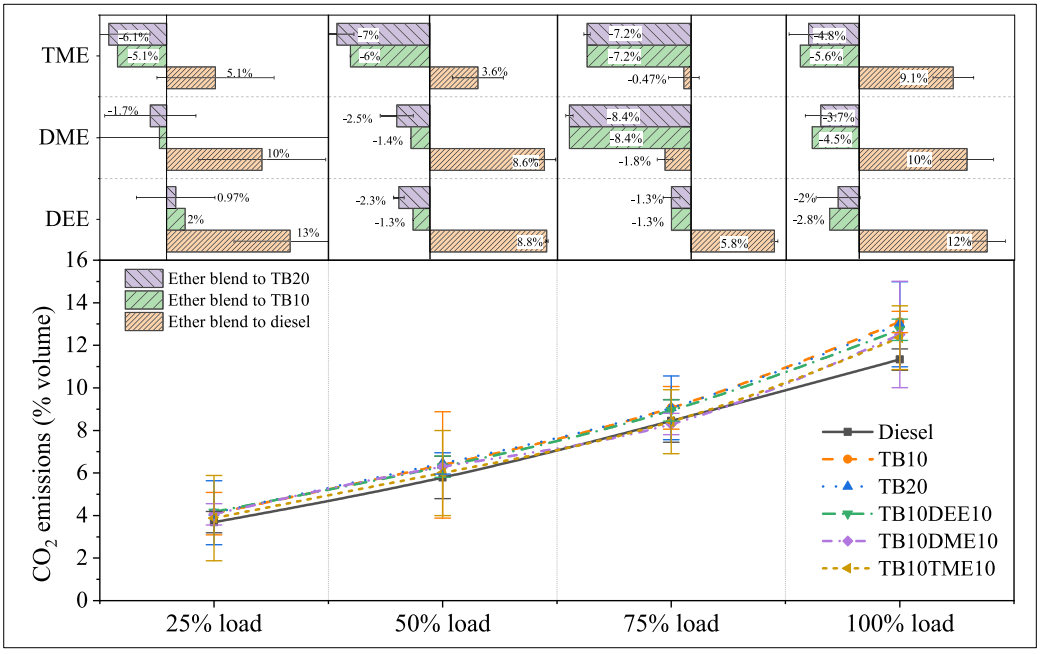

Fig. 6. Comparison of CO_2 emissions for the biodiesel and ether blends with diesel, TB10 and TB20.

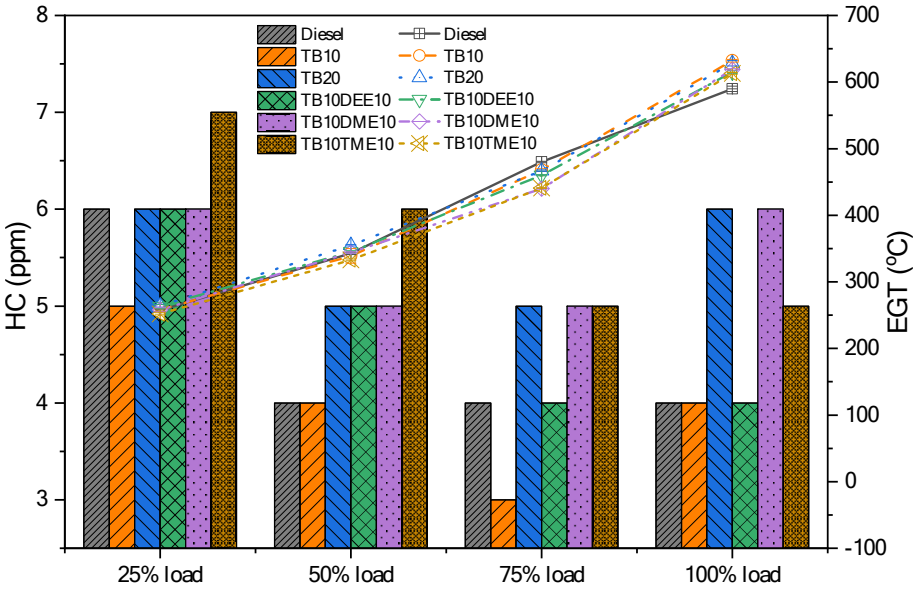

Fig. 7. Variation of HC emissions and EGT with respect to loads.

CO_2 at higher loads compared to diesel.

Adding ethers to the biodiesel has reduced the CO_2 emissions compared to TB10 and TB20. Compared to the DEE blend, DME and TME ether blends showed lower CO_2 emissions. At 75 % load, TB10DME10 and TB10DEE10 showed a 1.8 % and 0.47 % decrease in CO_2 than diesel. TB10TME10 has shown more significant CO_2 reductions at lower loads, for instance, 5.1 % and 6.1 % reduction in CO_2 compared to TB10 and TB20, respectively. At 75 % load condition, DME blends have shown an 8.4 % decrease in CO_2 compared to TB10 and TB20. On the other hand, DEE in the blend has shown increased CO_2 emissions. At 25 % load condition, the DEE blend showed an increase in CO_2 by 13 %, 2 %, and 0.97 % compared to diesel, TB10, and TB20, respectively. DEE has shown a 13 %, 8.8 %, 5.8 % and 12 % increase in CO_2 emissions compared to diesel at 25 %, 50 %, 75 % and 100 % load conditions, respectively. Krishnamoorthi and Malayalamurthi [75] and El-Zohairy et al. [76] observed increased CO_2 emissions with the DEE-biodiesel blends.

3.1.4. *Effect of biodiesel and ether blends on HC emissions*

Fig. 7 represents the exhaust gas temperature (EGT) vs the HC emissions with varying conditions for ether blends. HC emissions decreased with the increasing load to 75 % and then increased to 100 % load condition. This means that higher HC emissions are observed at a 25 % load and 100 % load. In the CI engine, the increase in HC is mainly

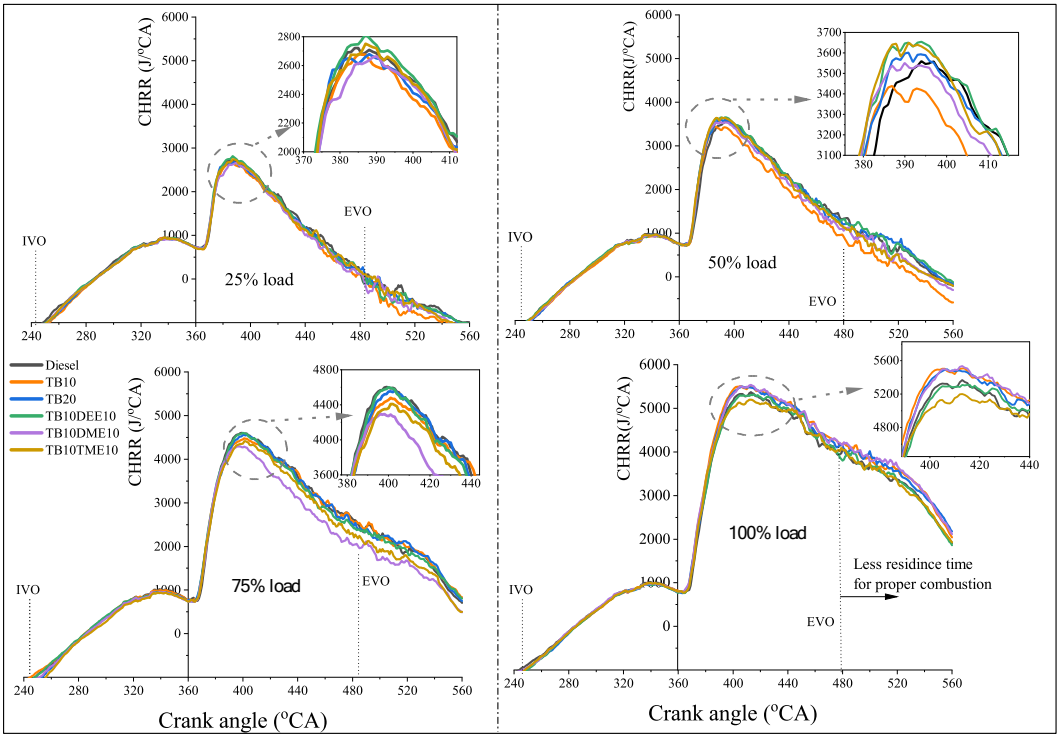

Fig. 8. Variation of CHRR at different loads for biodiesel and ether blends.

due to incomplete combustion. Incomplete combustion can occur due to various reasons. At 25 % load condition, higher HC is due to the lean mixture condition. At lean mixture conditions, flame propagation is low and will lead to partial oxidations and cause higher unburnt HC [77].

Interestingly, at 100 % load conditions, higher HC emissions are due to fuel-rich mixtures. For an overly rich mixture, the fuel either cannot mix with enough air or, even if mixed, does not have sufficient time to oxidise fully [78]. Moreover, HC emissions are also affected by the air–fuel ratio, poor combustion in crevice regions and poor combustion chamber design [79]. When gaseous HC interacts with sunlight, it produces photochemical smog, which poses a significant risk to the human respiratory system [80,81]. As shown in Fig. 7, the DME10 ether blend has shown increased HC emissions. This is because higher fuel consumption rates are noted for DME10 blend (3.12 kg/h) compared to DEE10 (3.04 kg/h) and TME10 blend (3.07 kg/h). Also, TB20 has shown increased HC emissions compared to TB10. This has also to do with the presence of a rich fuel mixture [82,83]. As can be seen from the BSFC plot (Fig. 11), there has been a significant difference in the fuel consumption rates between TB10 and TB20; hence, TB10 has shown lower HC emissions. Like CO emissions, higher temperatures are required to oxidize the HC emissions [77,84]. Hence, TB10 has shown lower HC emissions as it has higher heat release rates compared to other blends.

3.2. Effect of ethers on combustion parameters

3.2.1. Variation of CHRR with biodiesel and ether blends

Fig. 8 demonstrates the cumulative heat release rate (CHRR) of the diesel, biodiesel, and ether blends at varying loads. CHRR can imply the rate of fuel energy converted to useful energy [85]. The CHRR increased with the increasing load conditions, and this phenomenon was also observed in the study by Nabi et al. [86]. As can be seen, peak CHRR is noticed during the premixed combustion states. At 25 % load condition, higher CHRR is noticed for the TB10DEE10 with a peak value of 2816.72 J at 388 ℃A. Though TB10DEE10 has shown lower rates performance-wise, its higher CHRR signifies higher fuel consumption rates. At 25 % load, TB10DEE10 has shown higher fuel consumption than the other blended fuels. Similarly, TB10TME10 has also shown higher BSFC and, hence, the higher CHRR. However, in the case of TB10DME10, though the blend showed higher BSFC, the sudden rise in peak CHRR is low. This could be due to the uniform combustion of DME, which prohibited the sudden rise in HRR during the premixed combustion stage. Similar behavioral patterns in CHRR variations were also observed at other loads due to the BSFC.

At 50 % load again, TB10DEE10 and TB10TME10 showed peak HRR due to higher BSFC. On the other hand, TB10 has shown lower CHRR compared to other blends. But at 100 % load, Tucuma showed higher CHRR. This indicates that the TB10 blend has demonstrated its potential at full load conditions with lower BSFC value. However, the BSFC value of TB10 is 11 % higher than that of diesel at 100 % load condition. It could also be noticed that the sudden rise in peak values at 100 % load condition has led to better combustion by avoiding the unburnt hydrocarbons; however, due to limited oxygen content in the blend compared to other biodiesel blends, higher CO emissions can be noticed for TB10 at 100 % load condition. On the other hand, TB20 and TB10DME10 have shown higher BSFC at full load conditions; the sudden rise in peak CHRR is noticed, and the combustion is incomplete by the end of the exhaust valve opening time (EVO). Hence, higher HC emissions are seen in these two blends.

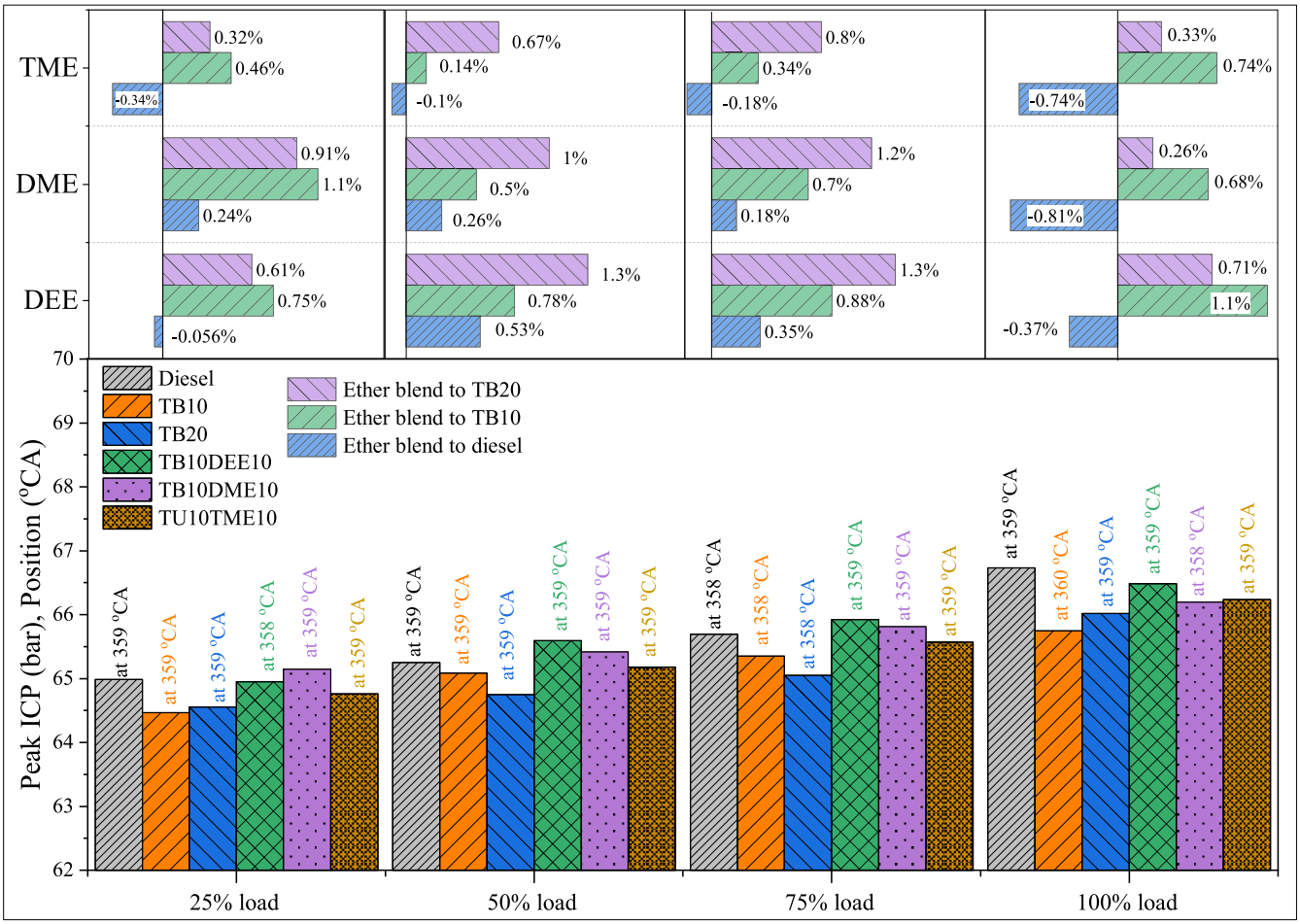

Fig. 9. Variation of peak ICP at different loads for biodiesel and ether blends.

3.2.2. Variation of peak in-cylinder pressure (ICP) rise rates with biodiesel and ether blends

Fig. 9 reveals the peak ICP rise rates of the biodiesel blends at varying load conditions. For Kubota V3300, the engine compression ratio is high (22.6:1), and by this, peak pressure can be marginally affected. A higher compression ratio can lead to shorter ignition delays and reduce peak pressure rates [87,88]. At 25 % load conditions, peak pressures were noticed in TB10DEE10 and TB10DME10 with values of 65.15 bar and 64.94 bar, respectively. As the pressure is directly proportional to the temperature, lower CO emissions are noticed for these two blends, implying higher oxidation rates. At the same time, peak pressures are also due to the rapid combustion occurrences inside the cylinder [89]. From the results, it is observed that there were no abnormal peak pressure changes, which can cause knocking. The peak pressure conditions were increased with the increase in load conditions. Though the calorific value for the TB10DME10 is lower, it showed higher ICP in 25 % load conditions. This is due to the presence of higher oxygen content and lower viscosity of the fuel, which has improved combustion. However, TB10DEE10 showed a higher ICP with 66.48 bar with the increasing load because of the higher calorific value than other blends. TB20 and TB10TME10 have shown lower peak pressures because of the higher densities that can cause wall wetting and fuel distribution problems. However, with the increase in load due to the rapid combustions, TB20 and TB10TME10 showed higher ICP and higher HC emissions.

3.2.3. Variation of the rate of pressure rise (ROPR) with biodiesel and ether blends

Fig. 10 presents the ROPR with biodiesel and ether blends at varying load conditions. RPR signifies the process occurring inside the chamber and is crucial for the efficient transfer of energy from the burned gases to the crankshaft [90,91]. It is observed from Fig. 10 that during the premixed combustion phase, a rapid ROPR occurred. It is due to the fast fuel burning after the injection, followed by the slow burning rate as the pressure variation is gradual in the diffusion stage. The rise in pressure impacts the formation of NO_x [92,93]. As discussed earlier, NO_x emissions increased at 75 % load and decreased at 100 % load. This can be related to Fig. 10, which shows that the RPR is high in the premixed zone at 75 % load condition and decreased at 100 % load condition. TB10TME10 has a lower rate of pressure rise at low loads, 0.91 dp/dθ due to the higher density of the blend. However, TB10TME10 showed higher ROPR at higher loads than TB10DEE10 and TB10DME10. At full load condition, TB20 showed a higher ROPR 1.30, followed by TB10 (1.17 dp/dθ), diesel (1.04 dp/dθ), TB10TME10 (1.03 dp/dθ), TB10DEE10 (0.91 dp/dθ) and TB10DME10 (0.54 dp/dθ). Ether blends have less ROPR than TB10 and diesel in all cases. In all the cases, an early rise in ROPR is noticed compared to diesel at the premixed combustion stage.

3.3. Effect of ether and biodiesel blends on performance parameters

3.3.1. Variation of ISFC and BSFC with biodiesel and ether blends

Fig. 11 demonstrates the variations of brake-specific fuel consumption (BSFC) and indicated specific fuel consumption (ISFC) for a wide

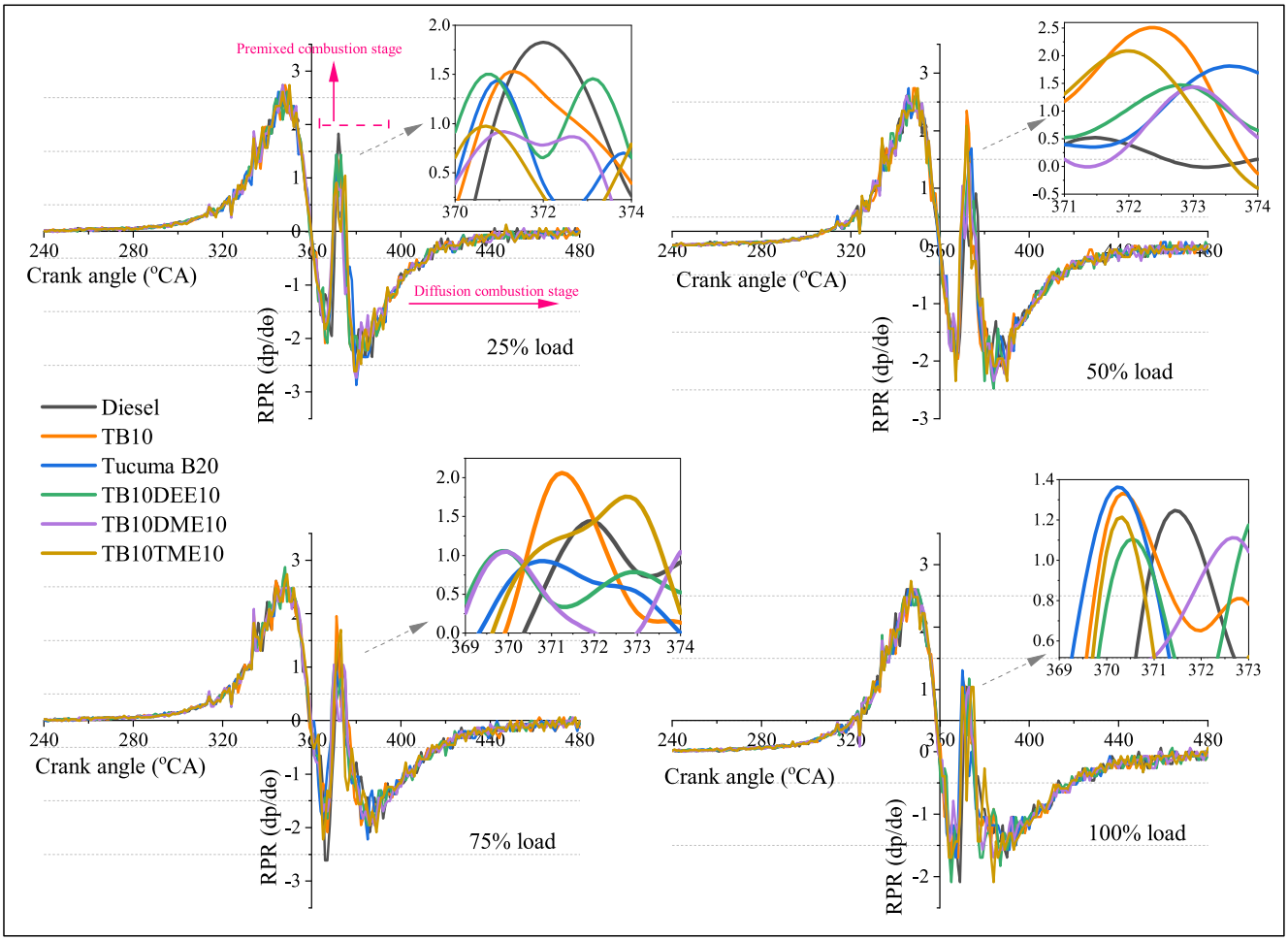

Fig. 10. Comparison of RPR at different loads for biodiesel and ether blends.

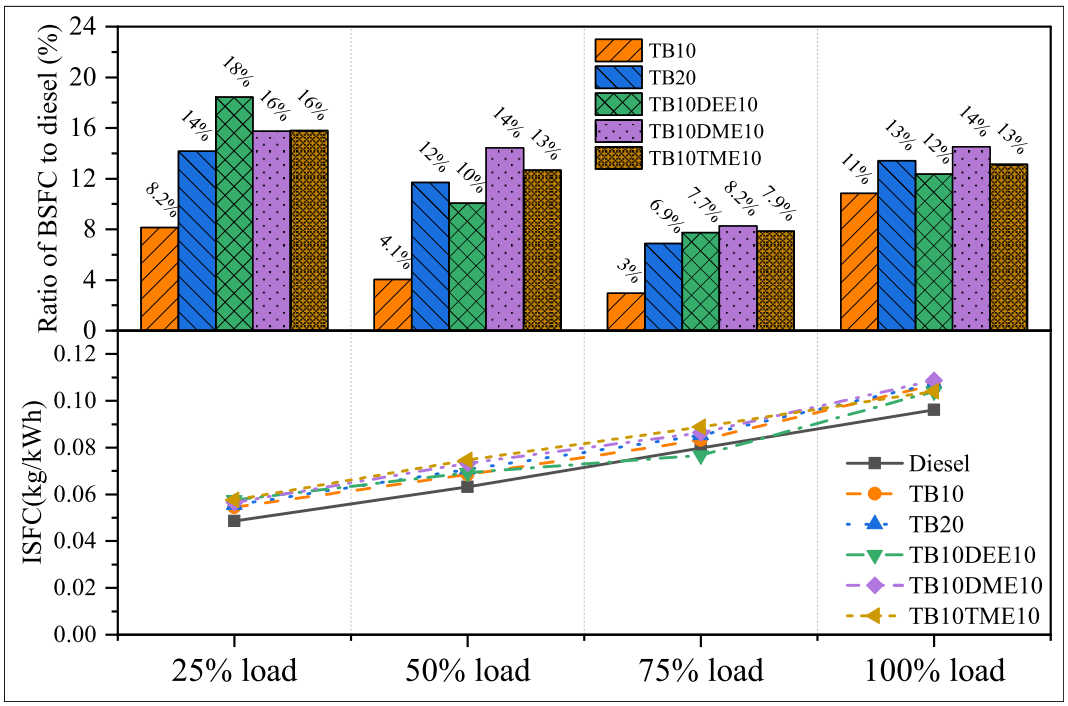

Fig. 11. Variation of ISFC and ratio of BSFC compared diesel at different loads.

range of oxygenated additives/fuels at a varying load range. It is well established that ISFC and BSFC have a reciprocal relationship with IP and BP, respectively. As seen in Fig. 11, BSFC and ISFC increase with increasing load. TB10 shows an 8.2 % increase in BSFC at 25 % load compared to diesel. 4.1 %, 3 %, and 11 % increase in BSFC using the same TB10 were realized at 50 %, 75 % and 100 % engine load, respectively. TB20 increases BSFC by 14 %, 12 %, 6.9 %, and 13 % at 25 %, 50 %, 75 % and 100 % loads, respectively. The increase in BP with three ether blends (TB10DEE10, TB10DME10, and TB10TME10) ranges from 7.7 to 18 %, 8.2–14 %, and 7.9–16 %, respectively. Like BSFC, ISFC was higher for all biodiesel and ether blends than diesel at all engine loading conditions. Though ethers support the combustion through

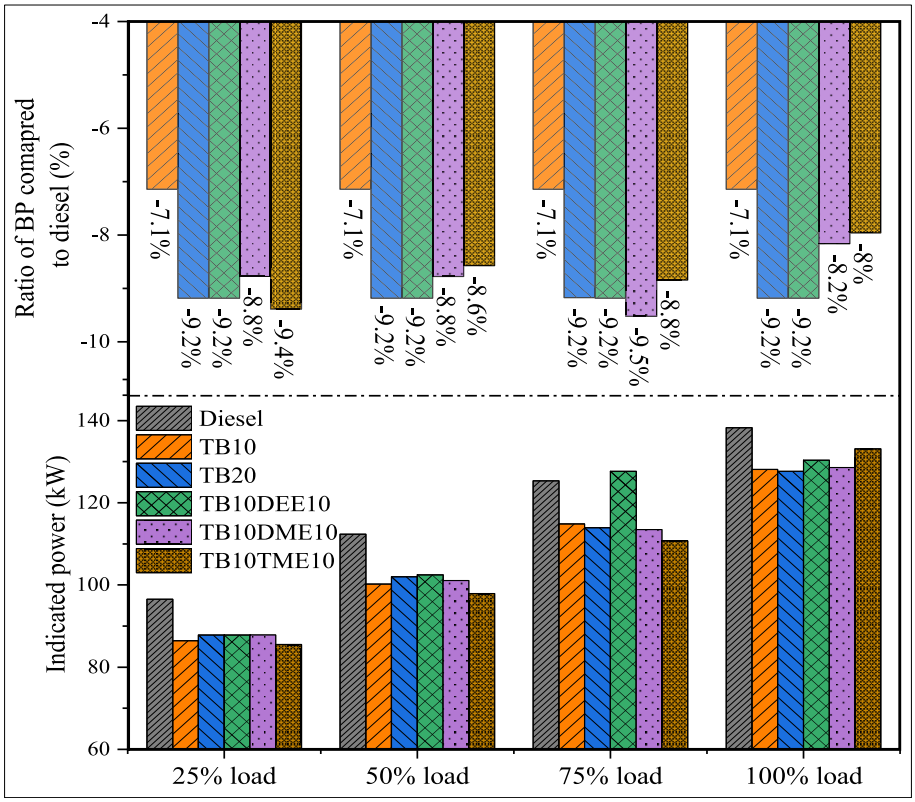

Fig. 12. Variation of IP and ratio of BP compared diesel at different loads.

higher oxygen content, the BSFC values are higher for the ether blends compared to diesel, TB10, and TB20. The main reason is due to the higher density of the ether blends. For instance, Jeevanantham et al. [94] observed a significant increase in BSFC by adding 5 % of DEE and methyl tertiary-butyl ether to the *Calophyllum Inophyllum* blend. Higher-density fuel was injected with more mass per unit volume, which reduced the air–fuel ratio and led to a higher fuel flow rate. In the case of TB10, the density of the blend is lower than all the other blends; hence, lower BSFC is noted with TB10. Another important factor is the lower calorific value, which is very low for the ethers. This might be beneficial to reduce the rapid combustion inside the cylinder but lead to more fuel consumption to obtain the desired rated power [95].

3.3.2. *Effect of engine load on engine power using diesel, biodiesel and ether blends*

The variations in engine output power (brake power, BP) and developed power in the cylinder (Indicated power, IP) using the same fuels and engine operating conditions are explained in Fig. 12 [45]. As can be seen from Fig. 12(a) and 12(b), the BP and IP with all ether blends are lower than diesel fuel. However, both powers show insignificant variations among the oxygenated additives blends. Compared to reference diesel, TB10 shows minimum variations in BP compared to diesel at all engine loading conditions. Interestingly, a maximum of 7.1 % lower BP was observed at all four engine loads with TB10. As anticipated, TB20, which has a lower energy content than TB10, shows a 9.2 % lower BP than diesel. The three ether blends, TB10DEE10, TB10DME10, and TB10TME10, show lower BP in the range of 9.2 to 9.5 %, 8.2 to 8.8 %, and 8 to 9.4 %, respectively. Concerning the IP, all blended fuels show lower IP than diesel. As can be seen from Fig. 12(b), IP is lower for TB10 than for TB20 and TB10DEE10. However, higher BP is noticed with the TB10 than the other biodiesel and ether blends. Several interesting factors involve the variation between BP and IP. The major factors for the variation in BP and IP are the frictional and lubricating losses. In internal combustion engines, the injected fuel can create such variations due to the differences in physical properties. For instance, the fuel with higher density can create higher frictional losses than the fuel with lower density. In the case of fuels TB20 and TB10DEE10, the density of the blend is high, and larger amounts of fuel were injected into the chamber [96]. The lubricating properties vary the fuel; hence, the blend IP is higher and BP is lower. Similar results with the variation in BP and IP between the fuels can also observed in the study by Deka et al. [97].

3.3.3. *Effect of engine load on thermal efficiency using diesel, biodiesel and ether blends*

The engine brake thermal efficiency (BTE) with respect to a wide range of engine loading conditions using a variety of tested fuels is displayed in Fig. 13(c). As seen in Fig. 13(c), the BTE increases with the increase in engine load, irrespective of the fuels. The BTEs get a

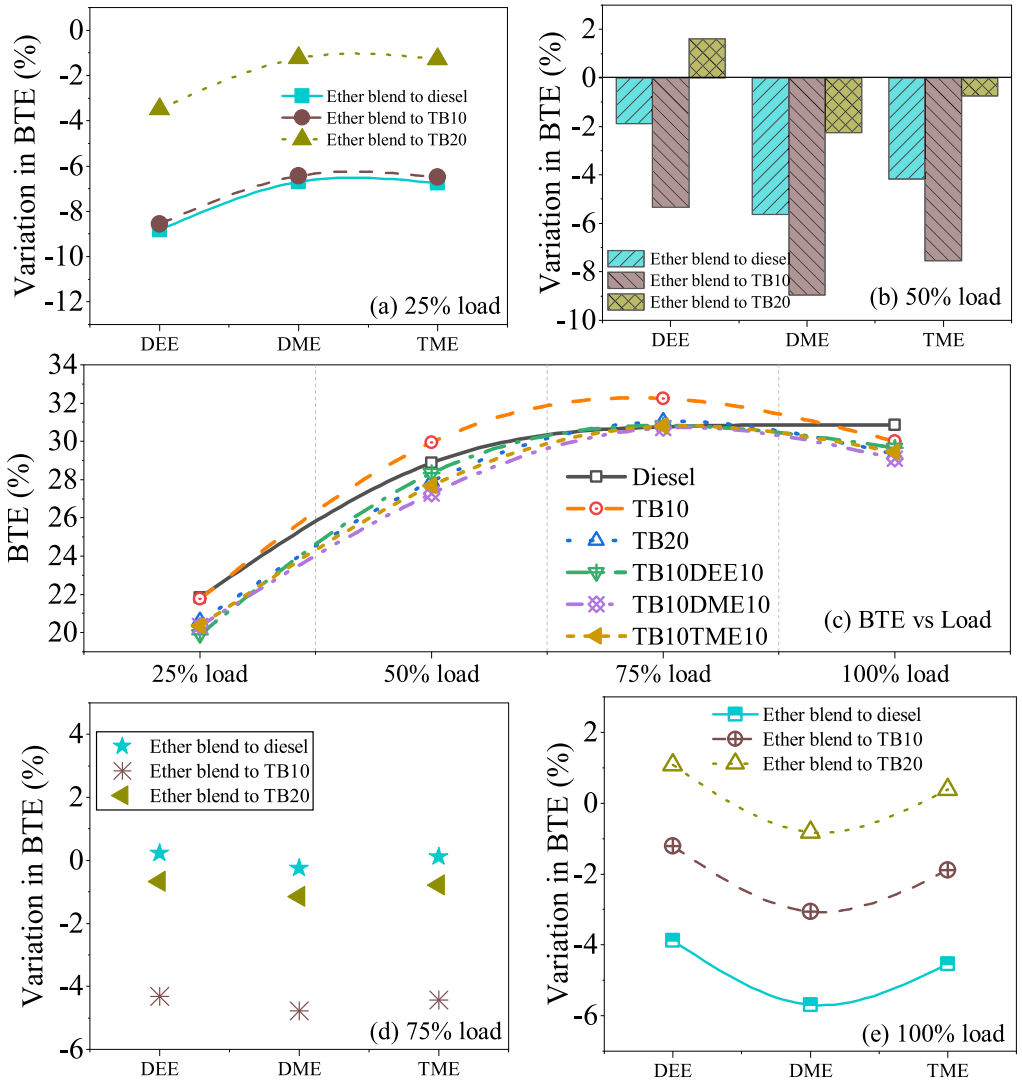

Fig. 13. Effect of ethers on BTE at different loads when compared to diesel, TB10, and TB20.

maximum at an engine load of around 75 % of the full and then decrease again. A similar trend is also reported in the study by Vural et al. [98]. TB10 has shown better BTE compared to diesel and other blended fuels. At 50 % and 75 % load conditions, TB10 demonstrated an increase in BTE by 3.7 % and 4.8 %, respectively, compared to diesel. However, at 100 % load, TB10 showed a 2.7 % decrease in BTE than diesel. This is due to the higher oxygen content of the TB10 compared to diesel, which has caused improved combustion. However, the higher oxygen content fuels such as TB20 and TB10-ether blends showed lower BTE because of the blend's lower calorific value and higher densities.

Fig. 13(a), 13(b), 13(d) and 13(e), shows the effect of TB10-ether blends when compared to the diesel, TB10 and TB20. Though ether blends have shown decreased emissions, BTE with the ether blends is quite poor compared to diesel and TB10. At lower loads (Fig. 13(a)), the TB10DEE10 blend has shown lower BTE compared to all the blends. This is mainly due to the higher BSFC of the blend compared to others at 25 % load condition. Abebe Debella et al. [12] observed lower BTE at low loads and increased BTE at high loads for the B20-DEE blends compared to B20. At 50 % load (Fig. 13(b)), all TB10-ether blends show lower BTE than diesel and TB10. The highest variations were found with ether blends to diesel, followed by ether blends to TB10. TB10DEE10 showed higher BSFC compared to TB20 at the 50 % load condition. It is interesting to note that at 75 % engine load (Fig. 13(d)), the variations of BTE are minimal, with ether blends to diesel, ether blends to TB10, and ether blends to TB20. When compared to diesel at 100 % engine load, ether blends showed inferior performance, while ether blends to TB20 had somewhat better performance. The reason for increasing the BTEs with DEE and TME at full engine load compared to TB20 needs further investigation. In most cases, the lower BTEs with ether blends to diesel, ether blends to TB10, and ether blends to TB20 are associated with the lower energy content in the ether-diesel, ether-TB10 and ether-TB20 blends. Regarding BTE with oxygenated fuels/additives, the current study aligns with the published articles [96,99,100].

4. Conclusion and recommendations

The study conducted the effect of oxygenated additives on biodiesel combustion to reduce NO_x and CO emissions. Three ethers: DEE, DME, and TME, were blended at 10 % by volume with the TB10 blend, and the results were compared with diesel, TB10, and TB20. The engine tests were carried out at a constant speed of 2400 rpm and variable the load condition. The following conclusions can be made from this study;

1) Adding three ethers to the TB10 blends has shown reduced NO_x compared to TB10. At 75 % load, ethers blend DEE, DME, and TME with TB10 showed reduced NO_x by 2.02 %, 6 %, and 6.6 %, respectively, compared to TB10. However, higher NO_x emissions were recorded with ether blends compared to diesel.
2) CO emissions are less with the TB10DEE10 and TB10DME10 ether blends than with diesel, TB10 and TB20. Overall, TB10DME10 showed lower CO than all the blends. At 100 % load, the addition of DME10 has reduced the CO by 22.3 %, 45 %, and 38 %, compared to diesel, TB10, and TB20, respectively. On the other hand, higher HC emissions are noted for the ether blends compared to diesel and TB10 due to the blend's higher density and lower calorific values.
3) TB10DEE10 has shown improved CHRR at 25 %, 50 %, and 75 % loads due to its low viscosity. However, at 100 %, TB10DME10 showed better CHRR due to increased combustion rates of high-density blend at higher load conditions.
4) Due to the lower calorific value of the ether blends compared to diesel, peak pressure values are lower for the biodiesel-ether blends than diesel. However, adding Ethers to the TB10 blend has increased the peak pressures compared to TB10 and TB20. At 100 % load conditions, ether blends TB10DEE10, TB10DME10, and TB10TME10 showed increased peak pressures by 1.1 %, 0.68 %, and 0.74 %, respectively, compared to the TB10 blend.
5) Adding ethers to the TB10 blend has significantly increased the BSFC compared to diesel and TB10. At 100 % load, TB10, TB20, TB10DEE10, TB10DME10, and TB10TME10 showed increase in BSFC by 11 %, 13 %,12 %, 14 % and 13 %, respectively compared to diesel.
6) A slight reduction in BTE is noted for ether blends compared to diesel. Among all the ether-TB10 blends, TB10DEE10 showed better BTE. A slight variation in BTE is noticed by −8%, −1%, 0.23 %, and −3.8 % for TB10DEE10 compared to diesel at loads 25 %, 50 %, 75 %, and 100 % loads, respectively compared to diesel.

Overall, the study found that adding DEE10 to TucumaB10 has shown better results in reducing CO, NO_x, and BSFC and improving BTE. The combustion of aspects of the ether blends needs more comprehensive understanding. A detailed computational fluid dynamics study will provide better understanding of the fuel behavior, particle dispersion and combustion formation inside the chamber. In addition, more studies are needed to assess the oxidative stability, tribological behavior and cold flow performance of the ether-biodiesel blends.

CRediT authorship contribution statement

Arun Teja Doppalapudi: Writing – original draft, Visualization, Software, Methodology, Investigation, Formal analysis. **Abul Kalam Azad:** Writing – review & editing, Visualization, Supervision, Resources, Project administration, Methodology, Investigation, Conceptualization. **Md Nurun Nabi:** Writing – review & editing, Formal analysis. **Mohammad G. Rasul:** Writing – review & editing. **Mohammad Masud Kamal Khan:** Writing – review & editing, Supervision.

Declaration of competing interest

The authors declare that they have no known competing financial interests or personal relationships that could have appeared to influence the work reported in this paper.

Data availability

Data will be made available on request.

References

[1] Dhileepan S, Viswanathan K, Esakkimuthu S, Balasubramanian D. Optimization of CRDI engine operating parameters using response surface methodology utilizing lemon peel oil biofuel enriched with hydroxy gas. Process Saf Environ Prot 2024;190:1506–19.
[2] Halder P, Azad AK. Chapter 7 - Recent trends and challenges of algal biofuel conversion technologies. In: Azad AK, Rasul M, editors. Advanced Biofuels. Woodhead Publishing; 2019. p. 167-179.
[3] M, V.B., M.M. K, A.P.R. G. Butanol and pentanol: the promising biofuels for CI engines – a review. Renew Sustain Energy Rev, 2017; 78: 1068-1088.
[4] Taipabu MI, Hsieh Y-L, Viswanathan K, Wu W. Organic ternary mixture separation and purification using chromatography: design, operation, and optimization. J Taiwan Inst Chem Eng 2023;153:105182.
[5] Taipabu MI, Viswanathan K, Mariyappan V, Kuo P-C, Aziz M, Wu W. Comparative analysis of hydrogen-rich syngas production from various feedstocks using bubbling fluidized bed. Process Saf Environ Prot 2024;189:1112–22.
[6] IEA, World Energy Outlook 2023, IEA, Editor. Paris; 2023.
[7] Cohen AJ, Brauer M, Burnett R, Anderson HR, Frostad J, Estep K, et al. Estimates and 25-year trends of the global burden of disease attributable to ambient air pollution: an analysis of data from the Global Burden of Diseases Study 2015. Lancet 2017;389(10082):1907–18.
[8] Kazemi Shariat Panahi H, Hosseinzadeh-Bandbafha H, Dehhaghi M, Orooji Y, Mahian O, Shahbeik H, et al. Nanotechnology applications in biodiesel processing and production: a comprehensive review. Renew Sustain Energy Rev 2024;192:114219.
[9] Marchetti AA, Knize MG, Chiarappa-Zucca ML, Pletcher RJ, Layton DW. Biodegradation of potential diesel oxygenate additives: dibutyl maleate (DBM), and tripropylene glycol methyl ether (TGME). Chemosphere 2003;52(5):861–8.
[10] Wang S, Viswanathan K, Esakkimuthu S, Azad K. Experimental investigation of high alcohol low viscous renewable fuel in DI diesel engine. Environ Sci Pollut Res 2021;28(10):12026–40.

[11] Manikandan G, Prabakaran R, Dhamodharan P, Kim SC, Joshuva GG, Boopathi M, et al. Performance analysis of a diesel engine using margosa oil ethyl ester-based biodiesel with diethyl ether as an oxygenated additive. Case Stud Therm Eng 2023;50:103496.

[12] Abebe Debella H, Ramayya Ancha V, Mekbib Atnaw S, Seyoum Zeleke D. Experimental study on performance and emissions from Prosopis Juliflora biodiesel blends with diethyl ether additives. Energy Convers Manage: X 2024;22:100581.

[13] El-Zohairy RM, Attia AS, Huzayyin AS, El-Seesy AI. Improving the biodiesel combustion and emission characteristics in the lean pre-vaporized premixed system using diethyl ether as a fuel additive. Fuel 2024;356:129614.

[14] Yesilyurt MK, Aydin M. Experimental investigation on the performance, combustion and exhaust emission characteristics of a compression-ignition engine fueled with cottonseed oil biodiesel/diethyl ether/diesel fuel blends. Energ Conver Manage 2020;205:112355.

[15] Swaminathan C, Sarangan J. A comparative study of performance and emission characteristics of biodiesel blends with diethylene glycol dimethyl ether as additive. Energy Sources Part A 2013;35(8):778–88.

[16] Bertoli C, D'Alessio J, Giacomo ND, Lazzaro M, Massoli P, Moccia V. Running light-duty DI diesel engines with wood pyrolysis oil. SAE Trans 2000:3090–6.

[17] Miyamoto N, Ogawa H, Nurun NM, Obata K, Arima T. Smokeless, low NOx, high thermal efficiency, and low noise diesel combustion with oxygenated agents as main fuel. SAE Trans 1998:171–7.

[18] Ren Y, Huang Z, Miao H, Jiang D, Zeng K, Liu B, et al. Effect of the addition of diglyme in diesel fuel on combustion and emissions in a compression– ignition engine. Energy Fuel 2007;21(5):2573–83.

[19] Zannis TC, Hountalas DT, Kouremenos DA. Experimental investigation to specify the effect of oxygenated additive content and type on DI diesel engine performance and emissions. SAE Trans 2004:166–79.

[20] Zhang Z-H, Balasubramanian R. Effects of oxygenated fuel blends on the composition of size-segregated engine-out diesel particulate emissions and on the toxicity of quasi-ultrafine particles. Fuel 2018;215:161–70.

[21] Yage D, Junjie Z, Chun Shun C, Xuelong M, Jinbao Z, Haiyong P, et al. Comparative study on combustion and particulate emissions for diesel-biodiesel and diesel-diglyme blends. Fuel 2022;313:122710.

[22] Nabi MN, Hustad JE. Experimental investigation of engine emissions with marine gas oil-oxygenate blends. Sci Total Environ 2010;408(16):3231–9.

[23] Mohammed AS, Atnaw SM, Ramaya AV, Alemayehu G. A comprehensive review on the effect of ethers, antioxidants, and cetane improver additives on biodiesel-diesel blend in CI engine performance and emission characteristics. J Energy Inst 2023;108:101227.

[24] Sun C, Liu Y, Qiao X, Ju D, Tang Q, Fang X, et al. Experimental study of effects of exhaust gas recirculation on combustion, performance, and emissions of DME-biodiesel fueled engine. Energy 2020;197:117233.

[25] Ashfaque Ahmed S, Elahi M, Soudagar M, Rahamathullah I, Sadhik Basha J, Yunus Khan TM, et al. Investigation of ternary blends of animal fat biodiesel-diethyl ether-diesel fuel on CMFIS-CI engine characteristics. Fuel 2023;332:126200.

[26] Doppalapudi AT, Azad AK, Khan MMK. Experimental investigation on diesel engine performance, combustion, and emissions characteristics with Tucuma and Ungurahui biodiesel blends. Fuel 2024;371:132161.

[27] Doppalapudi AT, Azad AK, Khan MMK. Exergy, energy, performance, and combustion analysis for biodiesel NOx reduction using new blends with alcohol, nanoparticle, and essential oil. J Clean Prod 2024;467:142968.

[28] Dumitrescu CE, Mueller CJ, Kurtz E. Investigation of a tripropylene-glycol monomethyl ether and diesel blend for soot-free combustion in an optical direct-injection diesel engine. Appl Therm Eng 2016;101:639–46.

[29] Ergen G. Comprehensive analysis of the effects of alternative fuels on diesel engine performance combustion and exhaust emissions: role of biodiesel, diethyl ether, and EGR. Therm Sci Eng Prog 2024;47:102307.

[30] Nabi MN, Rasul MG, Hazrat MA, Rashid F. Investigation of the effect of ether oxygenated additives on diesel engine performance, combustion, and exhaust emissions - an experimental approach. Energy 2024;304:132223.

[31] Azad AK, Jadeja AC, Doppalapudi AT, Hassan NM, Nabi MN, Rauniyar R. Design and simulation of the biodiesel process plant for sustainable fuel production. Sustainability 2024;16. https://doi.org/10.3390/su16083291.

[32] Viswanathan K, Huang J-M, Tsai T-H, Chang J-S, Wu W. Exploration of algal biorefinery frameworks: Optimization, quantification of environmental impacts and economics. Algal Res 2023;69:102903.

[33] Devaraj K, Mani Y, Rawoof SAA, Thanarasu A, Dhanasekaran A, Subramanian S. Feasibility of biodiesel production from waste cooking oil: lab-scale to pilot-scale analysis. Environ Sci Pollut Res 2020;27:25828–35.

[34] Encinar JM, Pardal A, Sánchez N. An improvement to the transesterification process by the use of co-solvents to produce biodiesel. Fuel 2016;166:51–8.

[35] Doppalapudi AT, Azad AK, Khan MMK, Oo AMT. Optimization and simulation of Tucuma and Ungurahui biodiesel process parameters and their effects on fuel properties. Energy Convers Manage: X 2024;24:100721.

[36] Doppalapudi AT, Azad AK. Advanced numerical analysis of in-cylinder combustion and NOx formation using different chamber geometries. Fire 2024;7. https://doi.org/10.3390/fire7020035.

[37] Azad AK, Halder P, Wu Q, Rasul MG, Hassan NMS, Karthickeyan V. Experimental investigation of ternary biodiesel blends combustion in a diesel engine to reduce emissions. Energy Convers Manage: X 2023;20:100499.

[38] Gupta HN. Fundamentals of internal combustion engines. PHI Learning Pvt. Ltd.; 2012.

[39] Azad AK, Rasul MG, Bhatt C. *Combustion and emission analysis of Jojoba biodiesel to assess its suitability as an alternative to diesel fuel*. Energy Procedia 2019;156:159–65.

[40] Mendera KZ, Spyra A, Smereka M. Mass fraction burned analysis. J KONES Internal Combustion Engines 2002;3(4):193–201.

[41] Yin P, Prabhu L, Saranya SN, Devanesan S, Alsahi MS, Anderson A, et al. Effects of Scenedesmus dimorphus, spirulina biodiesel, hydrogen and nanoparticles fuel blends on mass burn fraction, emission, noise and vibration characteristics. Fuel 2023;352:129010.

[42] Kale P. Combustion of biodiesel in CI engine. Int J Appl Res 2017;3:145–9.

[43] Akcay M, Ozer S. Experimental investigation on performance and emission characteristics of a CI diesel engine fueled with fusel oil/diesel fuel blends. Energy Sources Part A 2024;46(1):2600–15.

[44] Nabi MN, Rasul MG, Anwar M, Mullins BJ. Energy, exergy, performance, emission and combustion characteristics of diesel engine using new series of non-edible biodiesels. Renew Energy 2019;140:647–57.

[45] Viswanathan K, Ikhsan Taipabu M, Wu W. Novel Petit grain bitter orange waste peel oil biofuel investigation in diesel engine with modified fuel injection pressure and bowl geometry. Fuel 2022;319:123660.

[46] Azad AK, Doppalapudi AT, Khan MMK, Hassan NMS, Gudimetla P. A landscape review on biodiesel combustion strategies to reduce emission. Energy Rep 2023;9:4413–36.

[47] Doppalapudi AT, Azad AK, Khan MMK. Combustion chamber modifications to improve diesel engine performance and reduce emissions: a review. Renew Sustain Energy Rev 2021;152:111683.

[48] Avase S, Srivastava S, Vishal K, Ashok H, Varghese G. Effect of pyrogallol as an antioxidant on the performance and emission characteristics of biodiesel derived from waste cooking oil. Procedia Earth Planet Sci 2015;11:437–44.

[49] Khoa NX, Lim O. Comparative study of the effective release energy, residual gas fraction, and emission characteristics with various valve port diameter-bore ratios (VPD/B) of a four-stroke spark ignition engine. Energies 2020;13:1330.

[50] Nanthagopal K, Ashok B, Saravanan B, Patel D, Sudarshan B, Aaditya Ramasamy R. An assessment on the effects of 1-pentanol and 1-butanol as additives with Calophyllum Inophyllum biodiesel. Energ Conver Manage 2018;158:70–80.

[51] Özer S, Cenab C. Effects of adding waste oil ethylene glycol butyl ether to diesel fuel. Int J Automotive Sci Technol 2023;7(4):279–84.

[52] Sezer İ. Thermodynamic, performance and emission investigation of a diesel engine running on dimethyl ether and diethyl ether. Int J Therm Sci 2011;50(8):1594–603.

[53] Agarwal AK, Prashumn HV, Nath Mustafi N. Di-ethyl ether-diesel blends fuelled off-road tractor engine: Part-II: unregulated and particulate emission characteristics. Fuel 2022;308:121973.

[54] Rakopoulos DC, Rakopoulos CD, Giakoumis EG, Dimaratos AM. Characteristics of performance and emissions in high-speed direct injection diesel engine fueled with diethyl ether/diesel fuel blends. Energy 2012;43(1):214–24.

[55] Doppalapudi AT, Azad AK, Khan MM. Analysis of improved in-cylinder combustion characteristics with chamber modifications of the diesel engine. Energies 2023;16. https://doi.org/10.3390/en16062586.

[56] Sener R, Yangaz MU, Gul MZ. Effects of injection strategy and combustion chamber modification on a single-cylinder diesel engine. Fuel 2020;266:117122.

[57] Doppalapudi AT, Azad AK, Khan MMK. Advanced strategies to reduce harmful nitrogen-oxide emissions from biodiesel fueled engine. Renew Sustain Energy Rev 2023;174:113123.

[58] Khalife E, Tabatabaei M, Demirbas A, Aghbashlo M. Impacts of additives on performance and emission characteristics of diesel engines during steady state operation. Prog Energy Combust Sci 2017;59:32–78.

[59] Oh S, Park C, Oh J, Kim S, Kim Y, Choi Y, et al. Combustion, emissions, and performance of natural gas–ammonia dual-fuel spark-ignited engine at full-load condition. Energy 2022;258:124837.

[60] Kampa M, Castanas E. Human health effects of air pollution. Environ Pollut 2008;151(2):362–7.

[61] Chen G, Di L, Zhang Q, Zheng Z, Zhang W. Effects of 2, 5-dimethylfuran fuel properties coupling with EGR (exhaust gas recirculation) on combustion and emission characteristics in common-rail diesel engines. Energy 2015;93:284–93.

[62] Pan M, Huang R, Liao J, Jia C, Zhou X, Huang H, et al. Experimental study of the spray, combustion, and emission performance of a diesel engine with high n-pentanol blending ratios. Energ Conver Manage 2019;194:1–10.

[63] Raman LA, Deepanraj B, Rajakumar S, Sivasubramanian V. Experimental investigation on performance, combustion and emission analysis of a direct injection diesel engine fuelled with rapeseed oil biodiesel. Fuel 2019;246:69–74.

[64] Simsek S, Uslu S. Comparative evaluation of the influence of waste vegetable oil and waste animal oil-based biodiesel on diesel engine performance and emissions. Fuel 2020;280:118613.

[65] EdwinGeo V, Fol G, Aloui F, Thiyagarajan S, Jerome Stanley M, Sonthalia A, et al. Experimental analysis to reduce CO2 and other emissions of CRDI CI engine using low viscous biofuels. Fuel 2021;283:118829.

[66] Simsek S. Effects of biodiesel obtained from Canola, sefflower oils and waste oils on the engine performance and exhaust emissions. Fuel 2020;265:117026.

[67] Ma Q, Zhang Q, Liang J, Yang C. The performance and emissions characteristics of diesel/biodiesel/alcohol blends in a diesel engine. Energy Rep 2021;7:1016–24.

[68] Esakki T, Rangaswamy SM, Jayabal R. An experimental study on biodiesel production and impact of EGR in a CRDI diesel engine propelled with leather industry waste fat biodiesel. Fuel 2022;321:123995.

[69] Kannan D, Pachamuthu S, Nabi MN, Hustad JE, Løvås T. Theoretical and experimental investigation of diesel engine performance, combustion and emissions analysis fuelled with the blends of ethanol, diesel and jatropha methyl ester. Energ Conver Manage 2012;53(1):322–31.
[70] Panigrahi N, Mohanty MK, Mishra SR, Mohanty RC. Performance, emission, energy, and exergy analysis of a CI engine using mahua biodiesel blends with diesel. Int Scholarly Res Notices 2014;2014(1):207465.
[71] Simhadri K, Rao PS, Paswan M. Improving the combustion and emission performance of a diesel engine with TiO2 nanoparticle blended Mahua biodiesel at different injection pressures. Int J Thermofluids 2024;21:100563.
[72] Tan YH, Abdullah MO, Nolasco-Hipolito C, Zauzi NSA, Abdullah GW. Engine performance and emissions characteristics of a diesel engine fueled with diesel-biodiesel-bioethanol emulsions. Energ Conver Manage 2017;132:54–64.
[73] Nema VK, Singh A. Emission reduction in a dual blend biodiesel fuelled CI engine using nano-fuel additives. Mater Today Proc 2018;5(9):20754–9.
[74] Venu H, Appavu P. Experimental studies on the influence of zirconium nanoparticle on biodiesel–diesel fuel blend in CI engine. Int J Ambient Energy 2021;42(14):1588–94.
[75] Krishnamoorthi M, Malayalamurthi R. A review on effect of diethyl ether additive on combustion, performance and emission characteristics of a diesel and biodiesel/vegetable oil fuelled engine. Adv Natural Appl Sci 2016;10(7 SE):9–18.
[76] El-Zohairy RM, Attia AS, Huzayyin AS, El-Seesy AI. Effect of diethyl ether addition to waste cooking oil biodiesel on the combustion and emission characteristics of a swirl-stabilized premixed flame. Energ Conver Manage 2023;286:117052.
[77] Imtenan S, Varman M, Masjuki HH, Kalam MA, Sajjad H, Arbab MI, et al. Impact of low temperature combustion attaining strategies on diesel engine emissions for diesel and biodiesels: a review. Energ Conver Manage 2014;80:329–56.
[78] Turns SR. Introduction to combustion, vol. 287. New York, NY, USA: McGraw-Hill Companies; 1996.
[79] Raju VD, Kishore P, Nanthagopal K, Ashok B. *An experimental study on the effect of nanoparticles with novel tamarind seed methyl ester for diesel engine applications*. Energ Conver Manage 2018;164:655–66.
[80] Hosseinzadeh-Bandbafha H, Tabatabaei M, Aghbashlo M, Khanali M, Demirbas A. A comprehensive review on the environmental impacts of diesel/biodiesel additives. Energ Conver Manage 2018;174:579–614.
[81] Mofijur M, Ahmed SF, Ahmed B, Mehnaz T, Mehejabin F, Shome S, et al. Impact of nanoparticle-based fuel additives on biodiesel combustion: an analysis of fuel properties, engine performance, emissions, and combustion characteristics. Energy Convers Manage: X 2024;21:100515.
[82] Iodice P, Cardone M. Ethanol/gasoline blends as alternative fuel in last generation spark-ignition engines: a review on CO and HC engine out emissions. Energies 2021;14(13):4034.
[83] Liu X, Deng B, Fu J, Xu Z, Liu J, Li M, et al. The effect of air/fuel composition on the HC emissions for a twin-spark motorcycle gasoline engine: a wide condition range study. Chem Eng J 2019;355:170–80.
[84] Twigg MV. Progress and future challenges in controlling automotive exhaust gas emissions. Appl Catal B 2007;70(1–4):2–15.
[85] Dhar A, Agarwal AK. Performance, emissions and combustion characteristics of Karanja biodiesel in a transportation engine. Fuel 2014;119:70–80.
[86] Nabi MN, Hussam WK, Afroz HMM, Rashid AB, Islam J, Mukut ANMMI. Investigation of engine performance, combustion, and emissions using waste tire Oil-Diesel-Glycine max biodiesel blends in a diesel engine. Case Stud Therm Eng 2022;39:102435.
[87] Erman AG, Hellier P, Ladommatos N. The impact of ignition delay and further fuel properties on combustion and emissions in a compression ignition engine. Fuel 2020;262:116155.
[88] Thoo WJ, Kevric A, Ng HK, Gan S, Shayler P, La Rocca A. Characterisation of ignition delay period for a compression ignition engine operating on blended mixtures of diesel and gasoline. *Appl* Therm Eng 2014;66(1):55–64.
[89] Chen L, Pan J, Liu C, Shu G, Wei H. Effect of rapid combustion on engine performance and knocking characteristics under different spark strategy conditions. Energy 2020;192:116706.
[90] Cihan Ö. Experimental and numerical investigation of the effect of fig seed oil methyl ester biodiesel blends on combustion characteristics and performance in a diesel engine. Energy Rep 2021;7:5846–56.
[91] Singh M, Sheikh MY, Singh D, Rao PN. Combustion characteristics of single cylinder diesel engine fueled with blends of thumba biodiesel as an alternative fuel. Materials Science Forum. Trans Tech Publ; 2019.
[92] Gnanasekaran S, Saravanan N, Ilangkumaran M. Influence of injection timing on performance, emission and combustion characteristics of a DI diesel engine running on fish oil biodiesel. Energy 2016;116:1218–29.
[93] Shrivastava P, Salam S, Verma TN, Samuel OD. Experimental and empirical analysis of an IC engine operating with ternary blends of diesel, karanja and roselle biodiesel. Fuel 2020;262:116608.
[94] Jeevanantham AK, Nanthagopal K, Ashok B, Al-Muhtaseb AAH, Thiyagarajan S, Geo VE, Ong HC, Samuel KJ. Impact of addition of two ether additives with high speed diesel- Calophyllum Inophyllum biodiesel blends on NOx reduction in CI engine. Energy 2019;185:39–54.
[95] Ozer S, Doğan B. Thermodynamic analyzes in a compression ignition engine using fuel oil diesel fuel blends. Therm Sci 2022;26(4).
[96] Rahman MM, Rasul MG, Hassan NMS, Azad AK, Uddin MN. Effect of small proportion of butanol additive on the performance, emission, and combustion of Australian native first- and second-generation biodiesel in a diesel engine. Environ Sci Pollut Res Int 2017;24(28):22402–13.
[97] Deka P, Rahman M, Sharma S. Biodiesel production from chia seeds and comparison of b5, b10 and b20 blends to conventional diesel. 2022: 4; 728-739.
[98] Vural E, Ozel S, Ozer S. Coating of diesel engine with new generation ceramic material to improve combustion and performance. Therm Sci 2021;25(Spec. issue 1):101–10.
[99] Alwi A, Zulkifli NW, Sukiman NL, Yusoff A, Zakaria Z, Jamshaid M, et al. Evaluation of engine performance and exhaust emission characteristics in a diesel engine using isobutanol- Calophyllum inophyllum biodiesel-diesel ternary blends. Environ Sci Pollut Res Int 2019;26(12):11815–26.
[100] Nabi MN, Rasul MG. Influence of second generation biodiesel on engine performance, emissions, energy and exergy parameters. Energ Conver Manage 2018;169:326–33.